Bioelectrochemistry 73 (2008) 64–69

Contents lists available at ScienceDirect

Bioelectrochemistry

journal homepage: www.elsevier.com/locate/bioelechem

# Reaction of Cd(II)–Morin with dsDNA for biosensing of ssDNA oligomers with complementary, GCE-immobilized ssDNA

Shuyan Niu, Mingliang Wu, Sai Bi, Shusheng Zhang *

*Key Lab of Eco-chemical Engineering, Ministry of Education, College of Chemistry and Molecular Engineering, Qingdao University of Science and Technology, Qingdao 266042, PR China*

ARTICLE INFO

*Article history:*
Received 15 January 2008
Received in revised form 17 April 2008
Accepted 21 April 2008
Available online 27 April 2008

*Keywords:*
Electrochemical DNA biosensor
Morin
Cadmium
DNA hybridization detection
Differential pulse voltammetry

ABSTRACT

In this work, the complex cadmium(II)–morin was synthesized and its interaction with double-stranded salmon sperm DNA was studied by electrochemical methods on glassy carbon electrode (GCE). It was shown that Cd(II)–Morin with high electrochemical activity can intercalate into the double-helix DNA, and the binding stoichiometry and equilibrium dissociation constant according to the Hill model for cooperative binding were calculated to be 1.761 and $2.5\times10^{-5}$ M, respectively. Using Cd(II)–Morin as a novel hybridization indicator, the hybridization between the probe and its complementary and mismatched sequence was investigated by differential pulse voltammetry (DPV), which was to access the selectivity of the developed electrochemical DNA biosensor. The complementary target ssDNA could be quantified over the range from $2.69\times10^{-8}$ M to $9.16\times10^{-7}$ M with a linear correlation of 0.9971 and a detection limit of $9.30\times10^{-9}$ M. These results demonstrated that the Cd(II)–Morin indicator provides great promise for the rapid and selective measurement of the target DNA.



## 1. Introduction

Deoxyribonucleic acid (DNA) is one of the most important macromolecules with biological activity which plays a key role in the synthesis of proteins and gene expression. The detection of DNA has been widely used in the fields of diagnosis of genetic diseases, detection of infectious agents, different genetic expression, development of medicine, drug screening, food safety and environmental monitoring [1–6]. Electrochemical DNA biosensors based on nucleic acid hybridization have become a popular method for DNA sequence analysis owing to its good sensitivity, simplicity, accurate specificity and good compatibility [7–10].

Biosensors for DNA typically employ a single-stranded DNA probe sequence that is immobilized to the surface of an amperometric electrode. The detection methods of sequence-specific hybridization are either direct or indirect. For the direct detection protocol, the oxidation of guanine moiety in DNA strands eliminates the external labels (label-free detection), while indirect detection protocol is based on the incorporation an electroactive indicator [11,12] which has attracted a great deal of interests because it could generate a measurable electrochemical signal from the hybridization/recognition event. Moreover, as regards to the immobilization of DNA on the electrode surface and the presence of the high electroactive intercalators have become two leading directions for the construction of a more convenient and efficient DNA electrochemical biosensor [13,14], many kinds of indicators with different sensitivity and electroactivity have been developed for hybridization detection, such as anticancer agents, organic dyes, metal complex and so on. Seeking for novel hybridization indicators for DNA sequence analysis and detection, therefore, is of great significance.

Morin hydrate (2,(2,4-dihydroxyphenyl)-3,5,7-trihydroxy-4H-1-benzopyran-4-one), Scheme 1, a light yellowish natural plant dye, is known to have a broad pharmacological activity [15–20], such as antitumour [15], antioxidation [16], cardiovascular protection [17,18] and possibly even protective effects against chronic diseases [19,20]. Due to a convenient position of the 5OH and 4C=O as well as 3OH and 4C=O groups in a molecule, morin can easily form the chelate complex with ions of p-, d-, and f-electron metals [21]. Therefore, morin has been used as a colorimetric reagent for the spectrophotometric and fluorimetric determination of metal ions [22–24]. In general, compared with the ligand, the morin complex is considered to have a better biological activity due to its cooperative effectiveness, which results in the appealing studies of its antitumour activity. The synthesis [21,25] and investigation [26,27] of morin metal complex have been reported and different methods have been used to study its interaction with DNA [28–32], including fluorescence [28–30], phosphorescence [31], light scattering [32] and electrochemical analysis [28,33,34]. However, the complex of cadmium(II) with morin is rarely reported.

In the present paper, morin was chosen as a ligand for the synthesis of a novel cadmium(II) complex of $Cd(C_{15}H_9O_7)_2{\cdot}2H_2O$ [abbreviated by

* Corresponding author. Tel./fax: +86 532 84022750.
*E-mail address:* shushzhang@126.com (S. Zhang).

1567-5394/$ – see front matter © 2008 Elsevier B.V. All rights reserved.
doi:10.1016/j.bioelechem.2008.04.021

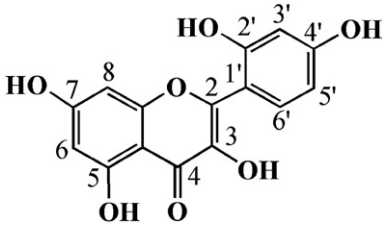

**Scheme 1.** The molecular structure of morin.

Cd($L_2$)]. The interaction between the Cd($L_2$) and double-stranded salmon sperm DNA was investigated by cyclic voltammetry (CV) and differential pulse voltammetry (DPV) methods. The experimental results show that Cd($L_2$) can bind with double-stranded DNA (dsDNA) to form a complex mainly by intercalation. Using Cd($L_2$) as an electrochemical indicator, a novel electrochemical DNA biosensor was developed after the accomplishment of hybridization of immobilized probe DNA with its complementary single-stranded DNA (ssDNA) on glassy carbon electrode (GCE). To the best of our knowledge, this work represents the first demonstration of Cd(II)–Morin in interaction with dsDNA and in the DNA biosensor as a hybridization indicator. The new electroactive indicator and electrochemical DNA biosensor are convinced to have promising applications in such fields as DNA detection, drug designing and diagnosis of disease.

## 2. Experimental

### 2.1. Apparatus

Infrared (IR) spectra were recorded on a Nicolet 510P FT-IR spectrophotometer. Elemental analysis was performed by a Perkin-Elmer 240 analyzer. All electrochemical measurements were carried out with Model CHI 832B Voltammetric Analyzer (CH Instruments, USA). A three-electrode system was employed with Pt wire as the auxiliary electrode, Ag/AgCl/KCl (saturated) as the reference electrode and GCE ($A$=0.071 $cm^2$) as the working electrode, respectively.

### 2.2. Reagents

The $Cd(C_{15}H_9O_7)_2{\cdot}2H_2O$ (Scheme 2) was prepared according to the literature [25]. Elementary analysis: Calc. (Found) for $Cd(C_{15}H_9O_7)_2{\cdot}2H_2O$: C 47.63 (48.00); H 2.97 (3.00) %; IR data (KBr disc, $cm^{-1}$, w, weak; s, strong; vs, very strong): $\nu$(O–H), 3428(vs); $\nu$(C=O), 1649(vs); $\nu$(C=C), 1549(vs); $\nu$(C–O–C), 1228(s); $\nu$(Ph), 1499(s); $\nu$($H_2O$), 697(s); $\nu$(Cd–O), 499(s).

Double-stranded salmon sperm DNA was purchased from Shanghai Huashun Biological Engineering Company ($A_{260}/A_{280}$>1.8). The concentration of dsDNA solution, expressed in moles of base pair, was determined by UV absorbance at 260 nm using the molar extinction coefficient ($\varepsilon$) of 13,200 $M^{-1}$ $cm^{-1}$. 1-ethyl-3-(3-dimethylaminopropyl) carbodiimide solution (EDC) and *N*-hydroxy succinimide solution (NHS) were purchased from Sigma and used without further purification. Three 24-base oligonucleotides were purchased from SBS Genetech Company (Beijing, China) with the following base sequences:

- probe ssDNA (denoted as $S_1$): 5′-GAG CGG CGC AAC ATT TCA GGT CGA-3′.
- Complementary target ssDNA (denoted as $S_2$): 5′-TCG ACC TGA AAT GTT GCG CCG CTC-3′.
- Non-complementary ssDNA to $S_1$ (denoted as $S_3$): 5′-TCG TCC TGA AAC GTT GCG CCT CTC-3′.

All oligonucleotides (100 μg $mL^{-1}$) were dissolved in Tris–EDTA buffer (TE, pH 8.0) and kept frozen. Other chemicals employed were all of analytical grade and ultrapure water was used throughout.

### 2.3. Electrochemical studies on the interaction between Cd($L_2$) and dsDNA

Appropriate amount of dsDNA and Cd($L_2$) was mixed and incubated in 0.20 M Tris–HCl buffer solution (pH 5.8) for 12 min. The interaction characterization of Cd($L_2$) with dsDNA was performed by CV, linear sweep voltammetry (LSV) and DPV method. For CV scanning, the potential scanning range was from 0.20 V to −1.0 V; the scanning rate was 0.15 V $s^{-1}$. For DPV, the initial potential was −1.0 V; the final potential was −0.60 V; the pulse scope was 0.004 V. For LSV, the potential scan was from −1.0 V to −0.40 V.

### 2.4. Preparation of the electrochemical DNA biosensor

#### 2.4.1. Covalent immobilization of probe ssDNA

The electrochemical DNA biosensor developed was based on the covalent immobilization of ssDNA on the modified GCE. Prior to the experiment, the GCE was firstly polished successively with 1.0 μm, 0.3 μm and 0.05 μm α-$Al_2O_3$ suspension. Afterwards, the electrode was oxidized at +0.50 V for 1 min in 50 mM phosphate buffer solution (PBS, pH 7.4). Subsequently, the surface activation of the above pretreated electrode was achieved by dropping 20 μL PBS containing 5.0 mM EDC and 8.0 mM NHS on it. After air-drying of this solution, the probe ssDNA ($S_1$) solution ($1.62\times10^{-5}$ M) was dropped on the activated electrode surface and allowed to dry under an infrared lamp. Then the electrode was rinsed with ultrapure water to eliminate the $S_1$ adsorbed.

#### 2.4.2. Hybridization reaction

The hybridization was carried out with the incubation of $S_1$-immobilized electrode in 20 mM Tris–HCl buffer solution (pH 7.0) containing complementary ssDNA ($S_2$) and non-complementary ssDNA ($S_3$), respectively, and allowed for 1 h at 37 °C with constant stirring. Afterwards, the electrode was dried at room temperature and successively rinsed with the same Tris–HCl buffer solution and ultrapure water to remove the residue $S_2$ or $S_3$ on the electrode surface.

#### 2.4.3. Intercalation of hybridization indicator

The accumulation of Cd($L_2$) on the hybridized electrode surface was performed by immersing the electrode into 0.20 M Tris–HCl buffer solution (pH 7.0) containing $6.54\times10^{-5}$ M Cd($L_2$) for 5 min at room temperature. Then, the electrode was washed with ultrapure water to remove the remnant Cd($L_2$) on the electrode surface.

### 2.5. Electrochemical detection

The electrochemical investigation of hybridization was carried out by DPV measurements in 0.20 M Tris–HCl buffer solution (pH 5.8), with potential scan from −1.0 V to −0.40 V. The peak related to the

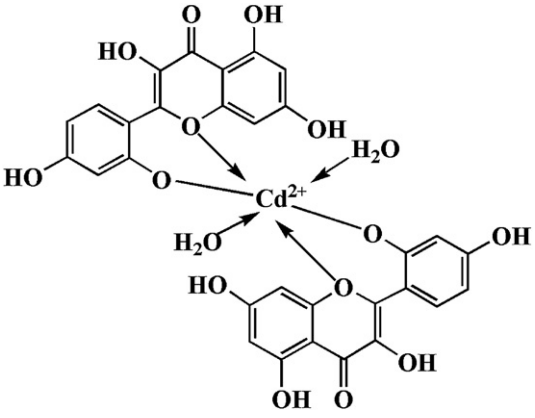

**Scheme 2.** Formula of Cd $(C_{15}H_9O_7)_2{\cdot}2H_2O$.

oxidation of $Cd(L_2)$ at −0.79 V was characterized as the electrochemical detection signal.

## 3. Results and discussion

### 3.1. Electrochemical interaction between $Cd(L_2)$ and dsDNA

#### 3.1.1. Electrochemical behaviors of $Cd(L_2)$ in the presence of dsDNA at bare GCE

Electrochemical behaviors of $Cd(L_2)$ and its interaction with dsDNA on the GCE at 25 °C were investigated. Fig. 1 shows DPVs obtained at a concentration of $6.54\times10^{-5}$ M $Cd(L_2)$ for bare GCE in the 0.20 M Tris–HCl buffer solution (pH 5.8) alone (curve a) or containing $2.15\times10^{-5}$ M dsDNA (curve b) and $5.62\times10^{-5}$ M dsDNA (curve c). It is observed that only one anodic peak ascribed to the oxidation of $Cd(L_2)$ appears at the potential of −0.79 V. The peak current is decreased and peak potential ($E_p$) shifted positively with the addition of dsDNA in Tris–HCl buffer, which strongly demonstrates the occurrence of the interaction between dsDNA and $Cd(L_2)$.

Bard [35] has reported the discrimination of binding modes between small molecules and DNA. If formal potential ($E^{\circ\prime}$) shifts to more negative value, the interaction mode is electrostatic binding. On the contrary, if $E^{\circ\prime}$ shifts to more positive value, the interaction mode is intercalative binding. Therefore, the interaction between $Cd(L_2)$ and dsDNA is attributed to the intercalative binding in this study. It is generally accepted that the planar aromatic heterocycle in morin plays a major intercalation role and inserts in the double-helix of dsDNA. Moreover, the decrease of peak current was also observed with the increasing concentration of dsDNA. As far as the peak current of anodic peak ($I_{pa}$) is concerned, the value of variational peak current is linear proportion to the concentration of dsDNA in the range of $3.63\times10^{-6}$–$5.62\times10^{-5}$ M, following equation below: $\Delta I_{pa}=1.67$ μA+{2.47 [DNA]/μM} μA.

Experimental conditions for the interaction between $Cd(L_2)$ and dsDNA, e.g., scan rate, reaction time, pH and iron strength were optimized. Fig. 2 shows the investigations between the different scan rates and $I_{pa}$ using LSV. In the presence and absence of dsDNA, the value of $I_{pa}$ is directly proportional to the scan rate $\nu$ (V/s) range from 0.14 V $s^{-1}$ to 0.38 V $s^{-1}$, suggesting an adsorption-controlled electrooxidation process of $Cd(L_2)$. Experiments to optimize the reaction time were also performed. The $I_{pa}$ reached a constant value with incubation dsDNA and $Cd(L_2)$ for 12 min, so 12 min was chosen as the reaction time. It was found that the value of $I_{pa}$ responded distinctly with the pH of the Tris–HCl buffer solution and a maximum peak current change before and after the addition of dsDNA was obtained at pH 5.8. Consequently, pH 5.8 was chosen as the optimum reactive pH. In the presence of dsDNA, when the ionic strength of the solution increased from 10 mM to 100 mM with additional amount of KCl, the $I_{pa}$ exhibited an unobviously increase and the peak potential had no shift to negative value. In general, the interaction modes of the complex with dsDNA are electrostatic and intercalative. If the ionic strength of the solution increases with a potassium salt, there will be a charge compensation of the nucleotide phosphates by the potassium ions, hindering the electrostatic binding to the complex [36]. The result presents that the ionic strength almostly has no effect on the interaction between $Cd(L_2)$ and dsDNA, corresponding with the fact of the intercalative interaction between $Cd(L_2)$ and dsDNA.

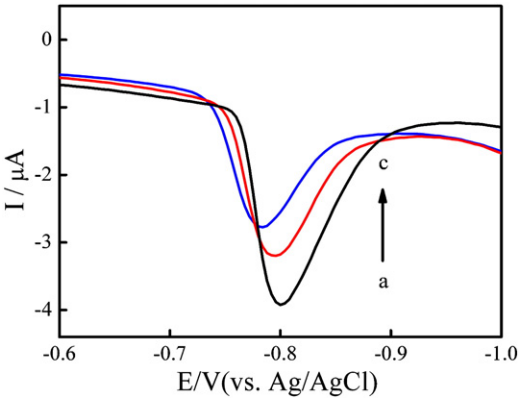


**Fig. 1.** DPVs of $Cd(L_2)$ in the absence and presence of dsDNA: (a) $6.54\times10^{-5}$ M $Cd(L_2)$, (b) (a)+$2.15\times10^{-5}$ M dsDNA, (c) (a)+$5.62\times10^{-5}$ M dsDNA.

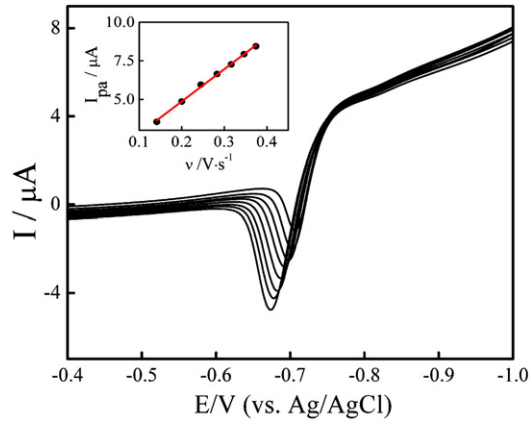


**Fig. 2.** LSVs of $Cd(L_2)$ in the different scan rates range from 0.14 V $s^{-1}$ to 0.38 V $s^{-1}$. Inset is the curve of peak currents versus the scan rates and the regression equation was $I_{pa}=0.673$ μA+{20.956[$\nu$/(V/s)]} μA with a correlation coefficient $r=0.9989$.

#### 3.1.2. Determination of the equilibrium dissociation constant and stoichiometric coefficient between $Cd(L_2)$ and dsDNA

The characteristic Hill parameters of the system for $Cd(L_2)$ and dsDNA were determined according to the literature [33,37]. It is assumed that dsDNA and $Cd(L_2)$ only produce a single complex dsDNA·$Cd(L_2)_m$. The stoichiometric coefficient, $m$, and the equilibrium dissociation constant $K$ between $Cd(L_2)$ and dsDNA refer to the reaction scheme (1) for all-or-none (Hill) cooperativity of multiple ligand binding:

$$\mathrm{dsDNA} + m\mathrm{Cd(L_2)} = \mathrm{dsDNA}\cdot\mathrm{Cd(L_2)}_m \quad (1)$$

The definition of equilibrium dissociation constant is as follows:

$$K^m = [\mathrm{Cd(L_2)}]^m\cdot[\mathrm{dsDNA}]/[\mathrm{dsDNA}\cdot\mathrm{Cd(L_2)}_m] = [\mathrm{Cd(L_2)}]^m(1-f)/f \quad (2)$$

Where the equilibrium dissociation constant $K$ is the reciprocal of the stability constant, ($K_{st}=1/K$), and $f$ as the fraction of intercalative complexation is defined as below:

$$f = [\mathrm{dsDNA}\cdot\mathrm{Cd(L_2)}_m]/[\mathrm{dsDNA}\cdot\mathrm{Cd(L_2)}_m]_{\max} = [\mathrm{Cd(L_2)}]^m/\{[\mathrm{Cd(L_2)}]^m + K^m\} \quad (3)$$

Then, the following logarithmic equation can be deduced from Eq. (3).

$$\log[f/(1-f)] = -m\log(K/M) + m\log\{[\mathrm{Cd(L_2)}]/M\} \quad (4)$$

Based on the above scientifically deduction, the fraction $f$ of dsDNA to which $Cd(L_2)$ is bound as dsDNA·$Cd(L_2)_m$, relative to the total dsDNA concentration in the supporting electrolyte are deduced in a similar way with Wang et al. [33] as follows:

$$[\mathrm{dsDNA}]_0 = [\mathrm{dsDNA}\cdot\mathrm{Cd(L_2)}_m]_{\max}.$$

where $[\mathrm{dsDNA}]_0$ is total concentration of dsDNA.

$$f = [\mathrm{dsDNA}\cdot\mathrm{Cd(L_2)}_m]/[\mathrm{dsDNA}]_0 \quad (5)$$

Mass conservation dictates that:

$$[\mathrm{dsDNA}] = [\mathrm{dsDNA}]_0 - [\mathrm{dsDNA}\cdot \mathrm{Cd(L_2)}_m]$$
$$[\mathrm{Cd(L_2)}] = [\mathrm{Cd(L_2)}]_0 - m[\mathrm{dsDNA}\cdot \mathrm{Cd(L_2)}_m] \quad (6)$$

and

$$I_{\mathrm{pa}} = k_1[\mathrm{Cd(L_2)}], \quad (7)$$

$$\Delta I_{\mathrm{pa}} = I_{\mathrm{pa}}(\mathrm{Cd(L_2)}_0) - I_{\mathrm{pa}}(\mathrm{Cd(L_2)}) \quad (8)$$

where [Cd(L$_2$)] is the free concentration of Cd(L$_2$) and $I_{pa}$(Cd(L$_2$)) is the anodic peak current of Cd(L$_2$) in the presence of dsDNA. Insertion of Eqs. (6) and (7) into Eq. (8) yields:

$$\Delta I_{\mathrm{pa}} = k_1\{[\mathrm{Cd(L_2)}]_0 - [\mathrm{Cd(L_2)}]\} = k_1 \cdot m \cdot [\mathrm{dsDNA}\cdot \mathrm{Cd(L_2)}_m] \quad (9)$$

and

$$\Delta I_{\mathrm{pa,\ max}} = k_1 \cdot m \cdot [\mathrm{dsDNA}]_0 \quad (10)$$

Where $\Delta I_{pa,\ max}$ is the maximum peak current change, obviously, [dsDNA·Cd(L$_2$)$_m$]$_{max}$=[dsDNA]$_0$ holds true. Insertion of Eqs. (9) and (10) into Eq. (5) yields:

$$f = \Delta I_{\mathrm{pa}}/\Delta I_{\mathrm{pa,\ max}} \quad (11)$$

Insertion of Eq. (11) into Eq. (4), the following equation can be yielded:

$$\log[\Delta I_{\mathrm{pa}}/(\Delta I_{\mathrm{pa,\ max}} - \Delta I_{\mathrm{pa}})] = -m\log(K/M) + m\log\{[\mathrm{Cd(L_2)}]/M\} \quad (12)$$

From Eq. (12), if dsDNA and Cd(L$_2$) only produced one single complex, the plot log [$\Delta I_{pa}$/($\Delta I_{pa,\ max}$−$\Delta I_{pa}$)] vs. log {[Cd(L$_2$)]/M} would become linear with the slope of $m$. The $K$ could be further deduced from the slope and the intercept.

The dependence of the anodic peak current of Cd(L$_2$) on the free concentration of Cd(L$_2$) in the absence (curve a) and presence (curve b) of dsDNA is shown in Fig. 3. The relationship between $\Delta I_{pa}$ and the free concentration of Cd(L$_2$) (curve c) is also displayed in Fig. 3. The numerical value of $\Delta I_{pa,\ max}$ can be obtained from the equation of the curve c with a kind of sigmoid.

As is shown in Fig. 4, the log [$\Delta I_{pa}$/($\Delta I_{pa,\ max}$−$\Delta I_{pa}$)] vs. log {[Cd(L$_2$)]/M} becomes linear with the slope of $m$. The results of $m$=1.761 and $K$=2.5×10$^{-5}$ M were obtained from Fig. 4.

### 3.2. The studies of DNA electrochemical sensor in the presence of Cd(L$_2$)

Based on the above discussion that Cd(L$_2$) can intercalate into the bases of dsDNA, it should be reasonable for the DNA biosensor

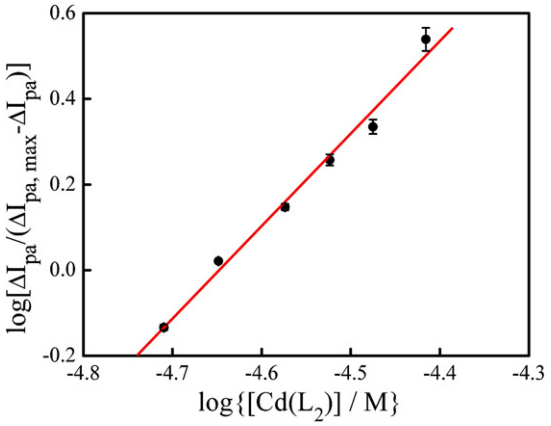


**Fig. 4.** Dependence of log {$\Delta I_{pa}$/($\Delta I_{pa,\ max}$−$\Delta I_{pa}$)} on log {[Cd(L$_2$)]/M}. The regression equation was log {$\Delta I_{pa}$/($\Delta I_{pa,\ max}$−$\Delta I_{pa}$)}=8.10+1.761 log {[Cd(L$_2$)]/M} with $r$=0.9801.

development with the use of Cd(L$_2$) as electrochemical hybridization. The hybridization reaction in the presence of Cd(L$_2$), of complementary ssDNA (S$_2$) with its immobilized probe ssDNA (S$_1$) on the GCE support, is as following:

$$\mathrm{c{-}S_2} + \mathrm{S_1(immobilized)} + \mathrm{Cd(L_2)} = \mathrm{ds{-}S_1S_2{-}Cd(L_2)} \quad (13)$$

where c-S$_2$ as complimentary ssDNA-Oligomer, S$_1$(immobilized) as probe ssDNA on the GCE and ds-S$_1$S$_2$-Cd(L$_2$) as product after hybridization and intercalation.

At the base of reaction scheme (13), the DNA electrochemical sensor was fabricated using Cd(L$_2$) as hybridization indicator and was investigated as follows.

#### 3.2.1. The electrochemical characterization of the biosensor fabrication

The electrochemical probe molecule $Fe(CN)_6^{3-}$/$Fe(CN)_6^{4-}$ was chosen to characterize the different modified electrodes. Fig. 5 shows the corresponding CVs for bare GCE (curve a), S$_1$ immobilized GCE (curve b) and hybridized (S$_1$–S$_2$) GCE (curve c) in 10 mM KCl solution containing 5.0 mM K$_3$Fe(CN)$_6$. Compared to the signal obtained on bare GCE, the peak currents of $Fe(CN)_6^{3-}$/$Fe(CN)_6^{4-}$ decreased significantly and the redox peak potential separation increased on S$_1$ modified GCE and hybridized (S$_1$–S$_2$) GCE, indicating that the diffusion of $Fe(CN)_6^{3-}$/$Fe(CN)_6^{4-}$ to the modified electrodes surface was largely inhibited due to the electrostatic repulsion between negative $Fe(CN)_6^{3-}$/$Fe(CN)_6^{4-}$ ions species and negative charged phosphate acid bone of ssDNA or dsDNA on the electrodes surface. It evidently reveals that the immobilization of probe ssDNA and

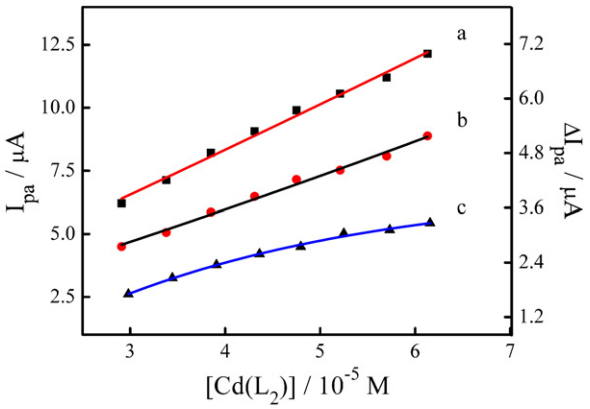


**Fig. 3.** Curves of anodic peak current of Cd(L$_2$) ($I_{pa}$), and $\Delta I_{pa}$ versus free concentration of Cd(L$_2$). (a) [dsDNA]: 0; (b) [dsDNA]: 2.86×10$^{-7}$ M; (c) $\Delta I_{pa}$=$I_{pa,\ a}$−$I_{pa,\ b}$.

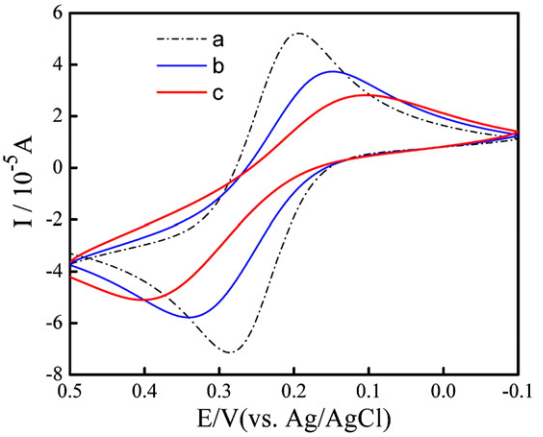


**Fig. 5.** The CVs of K$_3$Fe(CN)$_6$ on different electrodes (a) bare GCE; (b) S$_1$/GCE; (c) S$_1$–S$_2$/GCE.

further hybridization with complementary target ssDNA could be successively achieved with our advised procedures.

*3.2.2. The selectivity of the biosensor fabrication*

The selectivity of constructed electrochemical DNA biosensor with Cd($L_2$) as indicator was investigated by DPV. Fig. 6 shows the representative DPVs obtained in Tris–HCl buffer solution (pH 5.8) using $S_1$-modified GCE (curve a), $S_1$–$S_3$ hybridized GCE (curve b) and $S_1$–$S_2$ hybridized GCE (curves c, d and e) respectively as working electrode. Each measurement was performed after Cd($L_2$) was accumulated.

It could be seen from Fig. 6 that there is almost no DPV peak response of Cd($L_2$) for probe ssDNA modified electrode (curve a in Fig. 6). This demonstrates that just a negligible small amount of Cd($L_2$) could be accumulated onto electrode surface by electrostatic interaction with $S_1$.

The incubation with complementary target ssDNA yields an obviously increased peak current of Cd($L_2$) at about −0.79 V, and the peak currents in DPV responses at the complementary target ssDNA concentration of $1.62\times10^{-7}$ M, $6.23\times10^{-7}$ M and $9.16\times10^{-7}$ M were 0.23 μA, 0.47 μA and 0.64 μA, respectively (curve c, d and e in Fig. 6). The incubation with complementary target ssDNA yields a significantly increased peak current. The increased peak current indicates the successful intercalation of Cd($L_2$) into the base pairs of the dsDNA formed by $S_1$–$S_2$ target-specific hybridization, as is shown in the reaction scheme (13).

Additionally, no voltammetric response was detected in curve b for $S_1$–$S_3$ hybridized GCE. As we know, no base pair of the dsDNA was formed because $S_3$ was non-complementary to $S_1$. As a result, no Cd ($L_2$) was accumulated on the surface of electrode.

Conclusively, the above research strongly proves that Cd($L_2$) could interact with duplex DNA by major intercalation and the complementary target ssDNA could be readily recognized with immobilized probe ssDNA on the electrode surface with Cd($L_2$) utilized as a novel electrochemical indicator.

*3.2.3. The sensitivity of the biosensor fabrication*

The sensitivity of the fabricated DNA electrochemical sensor was studied by the different concentration of target ssDNA ($S_2$) complementary to the probe ssDNA ($S_1$) immobilized on GCE. As is shown in Fig. 7, the different anodic peak currents obtained in DPV measurement increases with the increasing concentration of $S_2$. The value of peak current is linear with the concentration of $S_2$ over the range from $2.69\times10^{-8}$ M to $9.16\times10^{-7}$ M. Thus, a detection limit of $9.30\times10^{-9}$ M of the target ssDNA could be estimated using $3\sigma$ (where $\sigma$ is the standard deviation of the blank solution, $n=11$).

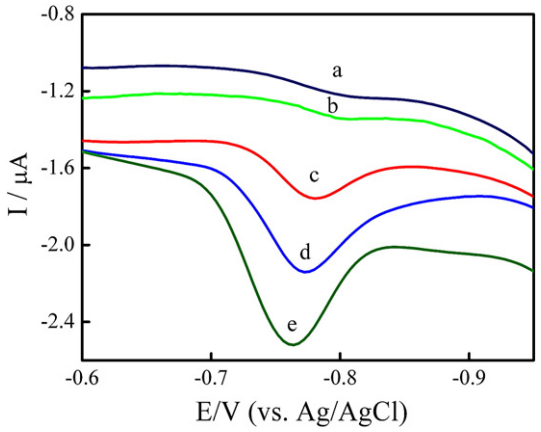


**Fig. 6.** The DPVs of different GCEs in Tris–HCl buffer solution (a) $S_1$/GCE (b) $S_1$–$S_3$/GCE; where the concentration of $S_3$ was $1.62\times10^{-7}$ M, (c) (d) (e) $S_1$–$S_2$/GCE, where the concentration of $S_2$ was $1.62\times10^{-7}$ M, $6.23\times10^{-7}$ M and $9.16\times10^{-7}$ M respectively.

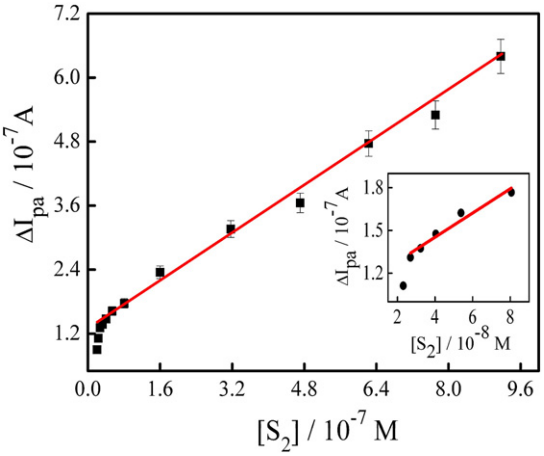


**Fig. 7.** The value of variational peak current ($\Delta I_{pa}$) versus concentration of target ssDNA ($S_2$). The regression equation was $\Delta I_{pa}=13.1$ μA+{5.41([$S_2$]/μM)} μA and the correlation coefficient $r$ was 0.9971.

*3.2.4. Regeneration and stability of the DNA biosensor*

Regeneration of the modified electrode was accomplished as follows: the hybridized surfaces of the electrodes were rinsed by hot (95 °C) ultrapure water for 5 min, rapidly cooled in an ice bath and tested the reusability of the repetitive hybridization biosensor. Following this procedure, the electrode response returned to its original signal that was obtained at the modified GCE surface prior to regeneration. The regenerated sensor produced a similar decrease of the DPV response when hybridized with the target ssDNA, demonstrating the regeneration and stability of the DNA biosensor. This regeneration of the modified GCEs with single-stranded oligonucleotides is useful for continuous monitoring of the target ssDNA in the future research.

## 4. Conclusions

The new electroactive indicator of cadmium(II)–morin was synthesized and its interaction with salmon sperm dsDNA was investigated using electrochemical methods. The binding stoichiometry $m=1.761$ and equilibrium dissociation constant $K=2.5\times10^{-5}$ M according to the Hill model for cooperative binding have been calculated. Moreover, using Cd($L_2$) as a novel electroactive indicator, the constructed electrochemical DNA biosensor could selectively detect the target ssDNA fragment. The surface hybridization of the immobilized ssDNA fragment with its complementary ssDNA fragment was proved by electrochemical methods. The target ssDNA could be quantified over a linear range from $2.69\times10^{-8}$ M to $9.16\times10^{-7}$ M with a detection limit of $9.30\times10^{-9}$ M. The developed electrochemical DNA biosensor based on the cadmium complex of morin would attain a promising in transducing DNA hybridization, drug designing and diagnosis of diseases.

## Acknowledgements

This work was supported by the National Natural Science Foundation of China (No.20775038), the Natural Science Foundation of Shandong Province (No. Y2007B31) and the Technical Development Project of Qingdao (06-3-1-4-yx).

## References

[1] U. Landergren, R. Kaiser, C.T. Caskey, L. Hood, DNA diagnostics-molecular techniques and automation, Science 242 (1988) 229–237.
[2] O.S. Frankfurt, A. Krishan, Enzyme-linked immunosorbent assay (ELISA) for the specific detection of apoptotic cells and its application to rapid drug screening, J. Immunol. Methods 253 (2001) 133–144.
[3] K.M. Millan, S.R. Mikkelsen, Sequence-selective biosensor for DNA based on electroactive hybridization indicators, Anal. Chem. 65 (1993) 2317–2323.

[4] S. Pankaj, G.K. Werner, Direct electrochemical detection of purine and pyrimidine based nucleotides with sinusoidal voltammetry, Anal. Chem. 69 (1997) 3552–3557.
[5] Y.W.L. Stratton, S. Roy, C.K. Se, DNA microarray technology in nutraceutical and food safety, Toxicol. Lett. 150 (2004) 29–42.
[6] V. Michaud, P. Gil, O. Kwiatek, S. Prome, L. Dixon, L. Romero, M.L. Potier, M. Arias, E.C. Hymann, F. Rogerf, G. Libeau, E. Albina, Long-term storage at tropical temperature of dried-blood filter papers for detection and genotyping of RNA and DNA viruses by direct PCR, J. Virol. Methods 146 (2007) 257–265.
[7] E.L.S. Wong, J.J. Gooding, Charge transfer through DNA: a selective electrochemical DNA biosensor, Anal. Chem. 78 (2006) 2138–2144.
[8] H.X. Chang, Y. Yuan, N.L. Shi, Y.F. Guan, Electrochemical DNA biosensor based on conducting polyaniline nanotube array, Anal. Chem. 79 (2007) 5111–5115.
[9] J. Wang, X. Cai, G. Rivas, H. Shiraishi, P.A.M. Farias, N. Dontha, DNA electrochemical biosensor for the detection of short DNA sequences related to the human immunodeficiency, Anal. Chem. 68 (1996) 2629–2634.
[10] P. Kara, B. Meric, A. Zeytinoglu, M. Ozsoz, Electrochemical DNA biosensor for the detection and discrimination of herpes simplex Type I and Type II viruses from PCR amplified real samples, Anal. Chim. Acta 518 (2004) 69–76.
[11] P. Kara, K. Kerman, D. Ozkan, B. Meric, A. Erdem, P.E. Nielsen, M. Ozsoz, Label-free and label based electrochemical detection of hybridization by using methylene blue and peptide nucleic acid probes at chitosan modified carbon paste electrodes, Electroanalysis 14 (2002) 1685–1690.
[12] M.H. Poumaghi-Azar, M.S. Hejazi, E. Alipour, Developing an electrochemical deoxyribonucleic acid (DNA) biosensor on the basis of human interleukine-2 gene using an electroactive label, Anal. Chim. Acta 570 (2006) 144–150.
[13] A. Erdem, Nanomaterial-based electrochemical DNA sensing strategies, Talanta 74 (2007) 318–325.
[14] D. Liu, R.K. Perdue, L. Sun, R.M. Crooks, Immobilization of DNA onto poly (dimethylsiloxane) surfaces and application to a microelectrochemical enzyme-amplified DNA hybridization assay, Langmuir 20 (2004) 5905–5910.
[15] V. Sivaramakrishnan, P. Shilpa, V. Kumar, S. Devaraj, Attenuation of *N*-nitroso-diethylamine-induced hepatocellular carcinogenesis by a novel favonol-morin, J. Virol. Methods 171 (2008) 79–88.
[16] T. Wu, K. Fung, J. Wu, C. Yang, J. Lo, R.D. Weisel, Morin hydrate inhibits azo-initiator induced oxidation of human low density lipoprotein, Life Sci. 58 (1996) 17–22.
[17] T.W. Wu, K. Fung, L.H. Zeng, J. Wu, A. Hempel, A.A. Grey, N. Camermano, Molecular properties and myocardial salvage effects of morin hydrate, Biochem. Pharmacol. 49 (1995) 537–543.
[18] L.D.S. Kok, Y.P. Wong, T.W. Wu, H.C. Chan, T.T. Kwok, K.P. Fung, Morin hydrate: a potential antioxidant in minimizing the free-radicals-mediated damage to cardiovascular cells by anti-tumor drugs, Life Sci. 67 (2000) 91–99.
[19] S. Fang, Y. Hou, W. Chang, S. Hsiu, P.L. Chaob, B. Chiang, Morin sulfates/glucuronides exert anti-inflammatory activity on activated macrophages and decreased the incidence of septic shock, Life Sci. 74 (2003) 743–756.
[20] V.K. Parihar, K.R. Prabhakar, V.P. Veerapur, K.I. Priyadarsini, M.K. Unnikrishnan, C.M. Rao, Anticlastogenic activity of morin against whole body gamma irradiation in Swiss albino mice, Eur. J. Pharmacol. 557 (2007) 58–65.
[21] E. Woznicka, M. Kopacz, M. Umbreit, J. Klos, New complexes of La(III), Ce(III), Pr(III), Nd(III), Sm(III), Eu(III) and Gd(III) ions with morin, J. Inorg. Biochem. 101 (2007) 774–782.
[22] L.A. Saari, W.R. Seltz, Immobilized morin as fluorescence sensor for determination of aluminum(III), Anal. Chem. 55 (1983) 667–670.
[23] M.J. Ahmed, J. Hossan, Spectrophotometric determination of aluminum by morin, Talanta 42 (1995) 1135–1142.
[24] E. Shamsa, A. Babaeib, M. Soltaninezhad, Simultaneous determination of copper, zinc and lead by adsorptive stripping voltammetry in the presence of morin, Anal. Chim. Acta 501 (2004) 119–124.
[25] Q. Zhang, L.F. Wang, X. Liu, Synthesis, characterization and antitumour properties of metal(II) solid complexes with morin, Transit. Met. Chem. 21 (1996) 23–27.
[26] P. Ryan, M.J. Hynes, The kinetics and mechanisms of the reactions of iron(III) with quercetin and morin, J. Inorg. Biochem. 102 (2008) 127–136.
[27] N. Binbuga, J.K. Hasty, S.R. Gwaltney, W.P. Henry, T.P. Schultz, Determination of the stability constants for the binding of sulfonated morin with $Fe^{2+}$, Inorg. Chim. Acta 360 (2007) 2339–2344.
[28] Y.M. Song, J.W. Kang, J. Zhou, Zh.H. Wang, X.Q. Lu, L.F. Wang, J.Zh. Gao, Study on the fluorescence spectra and electrochemical behavior of $ZnL_2$ and Morin with DNA, Spectrochim. Acta, Part A 56 (2000) 2491–2497.
[29] Y.M. Song, P.J. Yang, M.L. Yang, J.W. Kang, Sh.Q. Qin, B.Q. Lu, Spectroscopic and voltammetric studies of the cobalt (II) complex of Morin bound to calf thymus DNA, Transit. Met. Chem. 28 (2003) 712–716.
[30] Y.M. Song, J.W. Kang, Zh.H. Wang, X.Q. Lu, J.Zh. Gao, L.F. Wang, Study on the interactions between $CuL_2$ and Morin with DNA, J. Inorg. Biochem. 91 (2002) 470–474.
[31] J.M. Liu, T.L. Yang, F. Gao, L.X. Hu, H.X. He, Q.Y. Liu, Zh.B. Liu, X.M. Huang, G..H. Zhu, Determination of DNA by solid substrate room temperature phosphorescence enhancing method based on the Morin·$SiO_2$ luminescent nanoparticles–Pd system as a phosphorescence probe, Anal. Chim. Acta 561 (2006) 191–197.
[32] R.T. Liu, J.H. Yang, X. Wu, T. Wu, Resonance double frequency light scattering of the morin–nucleic acid–cetyltrimethylammonium bromide system and its analytical application, Anal. Chim. Acta 448 (2001) 85–91.
[33] F. Wang, Y.X. Xu, J. Zhao, Sh.Sh. Hu, Electrochemical oxidation of morin and interaction with DNA, Bioelectrochemistry 70 (2007) 356–362.
[34] J.W. Kang, Zh.F. Li, X.Q. Lu, Electrochemical study on the behavior of morin and its interaction with DNA, J. Pharm. Biomed. Anal. 40 (2006) 1166–1171.
[35] M.T. Carter, M. Rodriguez, A.J. Bard, Voltammetric studies of the interaction of metal chelates with DNA. 2. Tris-chelated complexes of cobalt(III) and iron(II) with 1,10-phenanthroline and 2,2'-bipyridine, J. Am. Chem. Soc. 111 (1989) 8901–8911.
[36] M.V. del Pozo, C. Alonso, F. Pariente, E. Lorenzo, DNA biosensor for detection of Helicobacter pylori using phen-dione as the electrochemically active ligand in osmium complexes, Anal. Chem. 77 (2005) 2550–2557.
[37] F. Qu, N.Q. Li, Y.Y. Jiang, Electrochemical studies of porphyrin interacting with DNA and determination of DNA, Anal. Chim. Acta 344 (1997) 97–104.